Theory of Optical Magneto-Absorption Effects in Semiconductors*

LAURA M. ROTH, BENJAMIN LAX, AND SOLOMON ZWERDLING
Lincoln Laboratory, Massachusetts Institute of Technology, Lexington, Massachusetts
(Received July 14, 1958)

The theory of the effect of a magnetic field on the optical absorption in semiconductors is developed on the basis of the effective-mass approximation. For simple parabolic conduction and valence bands and a direct transition which is allowed at $\mathbf{k}=0$, absorption peaks occur at energies above the zero-field gap. Since the selection rule for the transition is $\Delta n=0$ where n is the magnetic quantum number, the spacing between the peaks is the sum of the cyclotron frequencies for the two bands. For degenerate band edges, the spectrum is more complicated. A detailed treatment of the direct transition in germanium is given in which account is taken of the change in curvature of the bands away from $\mathbf{k}=0$ and the results are in good agreement with the experimental measurements of Zwerdling, Lax, Roth, and Button. The $\mathbf{k}=0$ conduction band mass is found to agree with predictions based on cyclotron resonance in the valence band. In addition, a gyromagnetic ratio for conduction electrons of -2.6 resulted from the calculations. The deviation from $g=2.0$ is due to spin-orbit interaction. In InSb the effect is much greater, the result being $g=-50$. These are consistent with experimental results. For bands in which the transition probability vanishes at $\mathbf{k}=0$, absorption peaks will also occur corresponding to $\Delta n=\pm 1$ but absorption edges occur for $\Delta n=0$. In the case of indirect transitions, the absorption does not exhibit oscillations but consists of a series of "steps" as has been observed in Ge by Zwerdling, Lax, Roth, and Button.

I. INTRODUCTION

In recent experiments,[1–4] the infrared absorption near the edge of the direct transition in semiconductors has been found to exhibit oscillations in the presence of a magnetic field. This oscillatory magneto-absorption effect has been observed in germanium, indium antimonide, indium arsenide, and gallium antimonide. The transmission minima observed are interpreted as due to transitions between magnetic levels of the valence and conduction bands at $\mathbf{k}=0$. In this paper the theory of the magneto-absorption effects will be worked out on the basis of the effective-mass approximation as developed by Luttinger and Kohn.[5]

We shall first treat an idealized semiconductor with two bands having a parabolic energy-momentum relation. We shall use this model to derive simple selection rules and the expected shape of the absorption as a function of photon energy, for direct and indirect transitions. Secondly, the case of the direct transition between a complex valence band, such as is found in germanium, and a parabolic conduction band, will be studied. The magnetic level structure of the valence band of germanium has been worked out in detail by Luttinger.[6] From this work the selection rules and statistical weights for the various transitions, as well as the energy levels, can be obtained. Using the results of microwave cyclotron resonance for the valence band parameters in germanium, the theoretical spectrum will be compared with experimental oscillatory magneto-absorption data. The anisotropy of the effect will be discussed, and the effect of polarization of the incident radiation will be examined.

The experimental results in InSb will also be interpreted. An interesting result in this case is the large magnetic spin splitting of the "s-like" conduction band because of the admixture of p-like states and the large spin-orbit interaction.

In analyzing the spectrum for the direct transition in germanium, it has been found that some of the absorption peaks are associated with exciton formation.[7] The magneto-absorption phenomena associated with this will be treated in detail in a later publication.

II. THEORY FOR SIMPLE BANDS

Let us consider first the problem of the optical absorption in a magnetic field of two simple bands separated by an energy gap, and both at the center of the Brillouin zone as shown in Fig. 1. We suppose the lower band, which is inverted, to be completely filled, and the upper band to be empty. In the absence of a magnetic field, the energies of the two bands are given as a function of the wave vector $\mathbf{k}$[8]:

$$\mathcal{E}_1=\mathcal{E}_1^0-k^2/2m_1, \quad \mathcal{E}_2=\mathcal{E}_2^0+k^2/2m_2, \tag{1}$$

where $\mathcal{E}_1^0$ and $\mathcal{E}_2^0$ are the band-edge energies and where m_1 and m_2 are the magnitudes of the effective masses of the two bands.

In the presence of a magnetic field the motion of the electrons can be described by the effective-mass approximation.[5] The energy for, e.g., band 1, is obtained in terms of the effective mass m_1 from the Schrödinger equation (neglecting spin)

$$\frac{1}{2m_1}\left(\mathbf{p}+\frac{e\mathbf{A}}{c}\right)^2 f_1(\mathbf{r})=(\mathcal{E}_1-\mathcal{E}_1^0)f_1(\mathbf{r}), \tag{2}$$

where $\mathbf{p}$ is the momentum operator $(1/i)\nabla$, $-e$ is the

* The research reported in this document was supported jointly by the Army, Navy, and Air Force under contract with the Massachusetts Institute of Technology.

[1] S. Zwerdling and B. Lax, Phys. Rev. **106**, 51 (1957).
[2] Zwerdling, Lax, and Roth, Phys. Rev. **108**, 1402 (1957).
[3] Zwerdling, Lax, Roth, and Button, preceding paper [Phys. Rev. **114**, 80 (1959)]; hereafter referred to as ZLRB.
[4] E. Burstein and G. S. Picus, Phys. Rev. **105**, 1123 (1957).
[5] J. M. Luttinger and W. Kohn, Phys. Rev. **97**, 869 (1955).
[6] J. M. Luttinger, Phys. Rev. **102**, 1030 (1956).
[7] Zwerdling, Roth, and Lax, Phys. Rev. **109**, 2207 (1958).
[8] We shall use units in which $\hbar=1$.

electronic charge, and $\mathbf{A}$ is the vector potential for the magnetic field. The zero-order wave function is given in terms of $f_1(\mathbf{r})$ by

$$\psi(\mathbf{r})=u_{10}(r)f_1(\mathbf{r}), \tag{3}$$

where $u_{10}(\mathbf{r})$ is the band-edge wave function[5] for band 1.[9]

The solution to Eq. (2) is well known.[10] If we choose the particular gauge for the magnetic field H in the z direction,

$$A_x=A_z=0, \quad A_y=-Hx, \tag{4}$$

then $f_1(\mathbf{r})$ can be written

$$f_1(\mathbf{r})=(L_yL_z)^{-\frac{1}{2}}\exp[ik_yy+ik_zz]\phi_n(x-ck_y/eH), \tag{5}$$

where ϕ_n is a one-dimensional harmonic oscillator wave function and where f_1 is normalized over the crystal, which we take to be a rectangular parallelepiped with sides L_x, L_y, L_z. Band 2 has wave functions of the same form as Eq. (5), and the energies for the two bands are given by

$$\begin{aligned}\mathcal{E}_1&=\mathcal{E}_1{}^0-\omega_{c1}(n+\tfrac{1}{2})-k_z{}^2/2m_1,\\ \mathcal{E}_2&=\mathcal{E}_2{}^0+\omega_{c2}(n+\tfrac{1}{2})+k_z{}^2/2m_2,\end{aligned} \tag{6}$$

where $\omega_{c1}=eH/m_1c$ is the cyclotron frequency for band 1, and similarly for band 2. Let us now let radiation fall on this simple semiconductor in the frequency range corresponding to the energy gap. The perturbation can be described by a time-varying electric field, whose space variation can be neglected, since the wavelength is long compared to the electronic wavelengths involved.[11,12] The perturbing term in the Hamiltonian is then

$$\mathcal{H}'=\frac{eE_0}{m}\left(\mathbf{p}+\frac{e\mathbf{A}}{c}\right)\cdot\frac{1}{2i\omega}[\boldsymbol{\varepsilon}\exp(i\omega t)-\boldsymbol{\varepsilon}^*\exp(-i\omega t)], \tag{7}$$

where m is the free electronic mass, ω is the frequency of the radiation, E_0 is the magnitude of the electric field, and $\boldsymbol{\varepsilon}$ is a unit vector in the direction of the field, which may be taken as complex in the case of circular polarization. By the usual methods of semiclassical radiation theory, the transition probability for the process in which an electron is raised from band 1 to band 2, and a photon is absorbed, is proportional to the square of the matrix element

$$\begin{aligned}M&=\frac{eE_0}{m\omega}\left\langle 1\left|\left(\mathbf{p}+\frac{e\mathbf{A}}{c}\right)\cdot\boldsymbol{\varepsilon}\right|2\right\rangle\\ &\cong\frac{eE_0}{m\omega}\int f_1{}^*(\mathbf{r})u_{10}{}^*(\mathbf{r})\left(\mathbf{p}+\frac{e\mathbf{A}}{c}\right)\cdot\boldsymbol{\varepsilon}f_2(\mathbf{r})u_{20}(\mathbf{r})d\mathbf{r}\end{aligned} \tag{8}$$

[9] That is, $u_{nk}(\mathbf{r})$ for $\mathbf{k}=0$ and $n=1$, where u_{nk} is the periodic part of the Bloch function $\exp[i\mathbf{k}\cdot\mathbf{r}]u_{nk}(\mathbf{r})$.

[10] L. Landau, Z. Physik **64**, 629 (1930).

[11] D. L. Dexter, *Proceedings of the Conference on Photoconductivity, Atlantic City, 1954*, edited by R. G. Breckenridge *et al.* (John Wiley & Sons, Inc., New York, 1956), p. 155.

[12] H. Brooks, *Advances in Electronics and Electron Physics*, edited by L. Marton (Academic Press, Inc., New York, 1955), Vol. 7, p. 85.

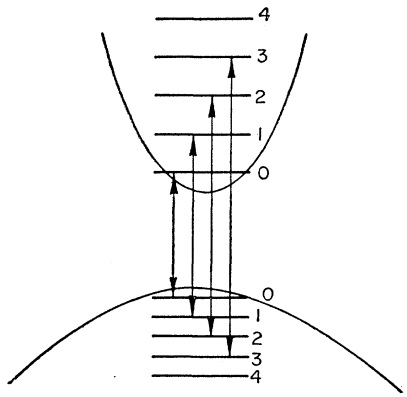

FIG. 1. Schematic diagram showing the magnetic levels, labeled by n ($k_z=0$) for two simple bands. The possible transitions are shown for the case in which the direct transition is parity allowed.

where we have used the zero-order wave functions of Eq. (3).

Since $f_1(\mathbf{r})$, $f_2(\mathbf{r})$ and $\mathbf{A}$ are slowly varying compared to the periodic functions u_{10} and u_{20}, we can treat f_1, f_2, and $\mathbf{A}$ as constant over a unit cell, and so break the integral up into an integral over a unit cell involving u_{10} and u_{20}, and an integral over the whole crystal involving f_1 and f_2. We assume the u's to be normalized to unit volume, and the f's over the whole crystal. Since the periodic functions for the two bands are orthogonal, the only nonvanishing term comes from applying the gradient to $u_{20}(\mathbf{r})$. This gives

$$\begin{aligned}M&=\frac{eE_0}{m\omega}\frac{1}{V_0}\int_{\text{cell}}u_{10}{}^*\mathbf{p}\cdot\boldsymbol{\varepsilon}u_{20}d\mathbf{r}\int_{\text{crystal}}f_1{}^*(\mathbf{r})f_2(\mathbf{r})d\mathbf{r}\\ &=\frac{eE_0}{m\omega}(\mathbf{p}_{12}\cdot\boldsymbol{\varepsilon})\int f_1{}^*(\mathbf{r})f_2(\mathbf{r})d\mathbf{r},\end{aligned} \tag{9}$$

where V_0 is the volume of the unit cell. M has been expressed in terms of the momentum matrix element $\mathbf{p}_{12}$ related to the oscillator strength for the transition. We shall assume that the two band edges have opposite parity so that $\mathbf{p}_{12}$ does not vanish.

Since $f_1(\mathbf{r})$ [Eq. (5)] does not depend on the effective mass, the corresponding function for band 2 has precisely the same form, so that the integral in Eq. (9) vanishes because of orthogonality unless $n=n'$, $k_y=k_y'$ and $k_z=k_z'$, where the primes refer to band 2. This is analogous to the selection rules conserving $\mathbf{k}$ in the absence of a magnetic field.

The absorption constant, α, is given by the relation[11,12]

$$\alpha=\frac{4\pi^2\omega}{ncE_0{}^2V}\sum_{1,2}|M|^2\delta(\omega-\mathcal{E}_2+\mathcal{E}_1), \tag{10}$$

where V is the volume of the crystal, n the index of refraction, and where the sum is over initial and final states, which will be paired off by the selection rules obtained from Eq. (9). The Dirac δ function insures

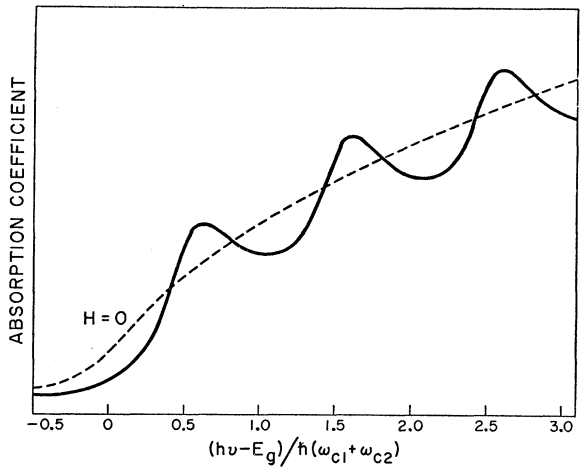

FIG. 2. Absorption coefficient as a function of energy for the bands shown in Fig. 1. The solid line shows the oscillatory magneto-absorption with $(\omega_{c1}+\omega_{c2})=5$.

conservation of energy. For the case of no magnetic field, the result is well known[11,12]:

$$\alpha_0=K\left(\frac{2m_1m_2}{m_1+m_2}\right)^{\frac{3}{2}}(\omega-\mathcal{E}_g)^{\frac{1}{2}},$$
$$K=2e^2(\mathbf{p}_{12}\cdot\boldsymbol{\varepsilon})/ncm^2\omega. \tag{11}$$

Here $\mathcal{E}_g=\mathcal{E}_2^0-\mathcal{E}_1^0$ is the energy gap.

The square-root factor determining the shape of the absorption edge comes in from the density of states near the edge of either band. In the magnetic case we have an absorption edge corresponding to each pair of Landau levels of magnetic quantum number n. Since the energy does not depend on k_y [Eq. (5)] each sub-band has a large degeneracy. This is obtained by restricting ck_y/eH, which is the x component of the center of the magnetic orbit, to values inside the crystal. The sum over pairs of initial and final states is then given by

$$\sum_{n,k_y,k_z}\delta[\omega-\mathcal{E}_2(n,k_z)+\mathcal{E}_1(n,k_z)]$$
$$=2L_yL_z\sum_n\int_{-(eH/2c)L_x}^{(eH/2c)L_x}\frac{dk_y}{2\pi}\int_0^\infty\frac{dk_z}{2\pi}\delta(\omega-\mathcal{E}_1+\mathcal{E}_2)$$
$$=(V/2\pi^2)(eH/c)\sum_n\left[\frac{d(\mathcal{E}_1-\mathcal{E}_2)}{dk_z}\right]^{-1}\Bigg|_{\omega=\mathcal{E}_1-\mathcal{E}_2}. \tag{12}$$

Thus we have appearing the density of states for a one-dimensional band. The result for α using Eq. (6) is then

$$\alpha_H=K\left(\frac{2m_1m_2}{m_1+m_2}\right)^{\frac{1}{2}}\frac{eH}{c}\sum_n(\omega-\omega_n)^{-\frac{1}{2}},$$
$$\omega_n=\mathcal{E}_g+(n+\tfrac{1}{2})(\omega_{c1}+\omega_{c2}), \tag{13}$$

where K is the same as in Eq. (11).

Equation (13) shows that for each sub-band absorption edge corresponding to the transition between Landau levels with $k_z=0$ there will be a peak in the absorption. The position of these peaks changes linearly with magnetic field. The peaks are of course broadened by collisions, which in the case of a semiconductor at room temperature are mainly due to phonons. This can be included phenomenologically by assuming a Lorentzian spread of energies of width $1/\tau$, in which case we find that for each peak we make the substitution

$$\frac{1}{(\omega-\omega_n)^{\frac{1}{2}}}\rightarrow\left\{\frac{\omega-\omega_n+[(\omega-\omega_n)^2+1/\tau^2]^{\frac{1}{2}}}{2[(\omega-\omega_n)^2+1/\tau^2]}\right\}^{\frac{1}{2}}. \tag{14}$$

The height of the line is proportional to $\tau^{\frac{1}{2}}$, and the peak is shifted to higher energy by an amount $(\tau\sqrt{3})^{-1}$ as can be seen by setting the derivative of Eq. (10) equal to zero. The shape of the oscillations for this type of broadening is shown in Fig. 2.

Figure 2 also shows that below the direct energy gap, the absorption edge is shifted and changes shape in a magnetic field. In the initial experiments on the effect of a magnetic field on the optical absorption,[13] this shift was measured by means of iso-transmission lines. The shift was not found to vary linearly with magnetic field, and in fact started out with a zero slope. Our simple model predicts such a result, as can be seen by looking at Eq. (13), in which we suppose a relaxation time has been put in. If we wish to evaluate α to first order in the magnetic field [or $(\omega_{c1}+\omega_{c2})$], we change the summation to an integration. However, the result of the integration is just Eq. (11), so that there is no change in α to first order in H. We must go therefore to second order in H before we obtain a shift, which is in agreement with experimental results. Since the discovery of the oscillations beyond the absorption edge, the motion of the transmission minima, which is a linear function of H, has been found to be a far more useful method for determining the shift of the band edge with field, and also, by means of extrapolation, the position of the band edge at zero field.

III. THEORY FOR COMPLEX BANDS

A. Direct Transitions

The simplified case worked out above serves to explain qualitatively many of the features to be found in the magneto-absorption near the direct gap in semiconductors. In this section, the transition probability is given for more general bands including the case of degenerate band edges and including spin-orbit interaction. We use the results of Luttinger and Kohn[3] for the effect of a magnetic field on the electrons near a band edge at $\mathbf{k}=0$. The energy levels and wave functions are obtained from the set of coupled Schrödinger-

[13] Burstein, Picus, Gebbie, and Blatt, Phys. Rev. **103**, 826 (1956); Zwerdling, Keyes, Foner, Kolm, and Lax, Phys. Rev. **104**, 1805 (1956).

like equations,

$$\sum_j[(\mathcal{E}_j^0-\mathcal{E})\delta_{ij}f_j(\mathbf{r})+\mathbf{P}\cdot\mathbf{D}_{ij}\cdot\mathbf{P}f_j(\mathbf{r})]=0, \quad (15)$$

where $\mathbf{P}=\mathbf{p}+e\mathbf{A}/c$, i and j run over the degenerate set at the band edge, and the dyadic $\mathbf{D}_{ij}$ is given by

$$\mathbf{D}_{ij}=\frac{1}{m}\delta_{ij}\mathbf{1}+\frac{1}{m^2}\sum_{\mu\neq i,j}\frac{\boldsymbol{\pi}_{i\mu}\boldsymbol{\pi}_{\mu j}}{\mathcal{E}_j^0-\mathcal{E}_\mu^0}, \quad (16)$$

$\mathbf{1}$ being the unit dyadic. Here $\boldsymbol{\pi}_{i\mu}$ is the modified momentum matrix element between bands i and μ at $\mathbf{k}=0$, which includes spin-orbit interaction:

$$\boldsymbol{\pi}_{i\mu}=\int u_{i0}(\mathbf{r})\left[\mathbf{p}-\frac{1}{4mc^2}(\nabla V\times\boldsymbol{\sigma})\right]u_{\mu 0}(\mathbf{r})d\mathbf{r}, \quad (17)$$

where V is the crystalline potential, and $\boldsymbol{\sigma}$ the Pauli spin vector.

The first-order wave functions are given in terms of the f's of Eq. (15) and the band-edge wave functions by

$$\psi=\sum_j f_j(\mathbf{r})u_{j0}(\mathbf{r})+\sum_{\nu\neq j}\left[\frac{1}{m}\frac{1}{\mathcal{E}_j^0-\mathcal{E}_\nu^0}\sum_i\boldsymbol{\pi}_{\nu j}\cdot\mathbf{P}f_j(\mathbf{r})\right]u_{\nu 0}(\mathbf{r}). \quad (18)$$

Using these wave functions, we can now give the matrix element for direct optical transitions between two bands, i.e., the generalization of Eq. (8). By treating the second part of Eq. (18) as small, the following result can be obtained:

$$M=\frac{eE_0}{m\omega}\left\{\left[\sum_{ip}\boldsymbol{\pi}_{jp}\cdot\boldsymbol{\varepsilon}\right]\int f_j^{*I}f_p^F d\mathbf{r}+\sum_{ip}\boldsymbol{\varepsilon}\cdot\left[\delta_{jp}\mathbf{1}+\frac{1}{m}\sum_{\mu\neq p}\frac{\boldsymbol{\pi}_{j\mu}\boldsymbol{\pi}_{\mu p}}{\mathcal{E}_p^0-\mathcal{E}_\mu^0}+\frac{1}{m}\sum_{\mu\neq j}\frac{\boldsymbol{\pi}_{\mu p}\boldsymbol{\pi}_{j\mu}}{\mathcal{E}_j^0-\mathcal{E}_\mu^0}\right]\cdot\int f_j^{*I}\mathbf{P}f_p^F d\mathbf{r}\right\}. \quad (19)$$

Here j runs over the degenerate set for band 1, and p for band 2, I and F stand for initial and final states. In the first term we are neglecting a quantity proportional to $eH/[mc(\mathcal{E}_p^0-\mathcal{E}_j^0)]$.

The first term in Eq. (19) vanishes unless bands 1 and 2 have opposite parity, and so is the result for transitions allowed at $\mathbf{k}=0$. Note that Eq. (19) justifies the use of the zero order wave function in the previous section, since the second term vanishes unless the two bands have the same parity. This latter term gives the results for transitions forbidden at $\mathbf{k}=0$, for which the absorption in the absence of the field[11,14] is proportional to $(\omega-\mathcal{E}_g)^{\frac{3}{2}}$. The selection rules for this case are determined by the integral in the second term of Eq. (19). In the case of simple parabolic bands such as were used in the previous section, we have $\Delta n=n'-n=0,\ \pm 1$. If we also suppose that the dyadic in Eq. (18) is a multiple C of the unit dyadic and that the radiation is isotropic, a simple result for α analogous to that in the previous section can be obtained:

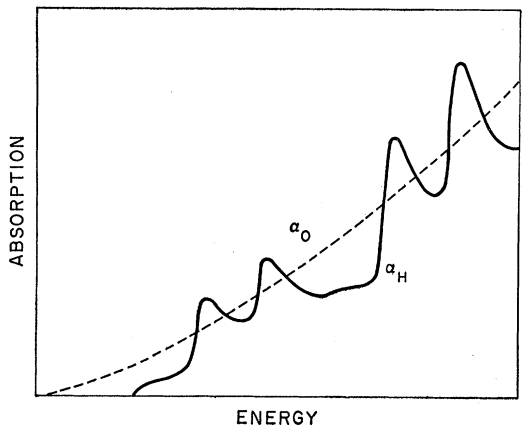

FIG. 3. Absorption coefficient as a function of energy for two simple bands when the transition is forbidden at $\mathbf{k}=0$. This was constructed for the case $\omega_{c2}=\frac{1}{3}\omega_{c1}$.

$$\alpha_0=K'\left(\frac{2m_1m_2}{m_1+m_2}\right)^{\frac{5}{2}}(\omega-\mathcal{E}_g)^{\frac{3}{2}},$$

$$K'=\frac{2e^2|C|^2}{3ncm^2\omega},$$

$$\alpha_H=3K'\left(\frac{2m_1m_2}{m_1+m_2}\right)^{\frac{3}{2}}\frac{eH}{c}\sum_{nn'}\left\{\tfrac{1}{3}(\omega-\mathcal{E}_{nn'})^{\frac{1}{2}}\delta_{nn'}+\tfrac{1}{6}(\omega_{c1}+\omega_{c2})\frac{n\delta_{n',n-1}+n'\delta_{n',n+1}}{(\omega-\mathcal{E}_{nn'})^{\frac{1}{2}}}\right\}, \quad (20)$$

$$\mathcal{E}_{nn'}=\mathcal{E}_g+\omega_{c1}(n+\tfrac{1}{2})+\omega_{c2}(n'+\tfrac{1}{2}).$$

We see in Eq. (20) that for $n'=n\pm 1$, there are peaks in the absorption. This is analogous to the transitions involved in cyclotron resonance. For $n'=n$ we have simply a series of absorption edges. The behavior of α as a function of energy is illustrated in Fig. 3. An analogous transition occurs between the three valence bands in germanium and has been analyzed for the nonmagnetic case by Kahn[15] assuming parabolic bands. (Note that for the valence bands with our sign convention, m_2 and ω_{c2} would be negative.) It should therefore be possible to observe oscillations in the magneto-absorption between the valence bands, although it appears from the complexity of the spectrum

[14] In the case of semiconductors, such as InSb, which lack inversion symmetry, it is possible to have both terms in Eq. (19), as has been pointed out by Blatt, Wallis, and Burstein, Bull. Am. Phys. Soc. Ser. II, 2, 141 (1957).

[15] A. H. Kahn, Phys. Rev. 97, 1647 (1955).

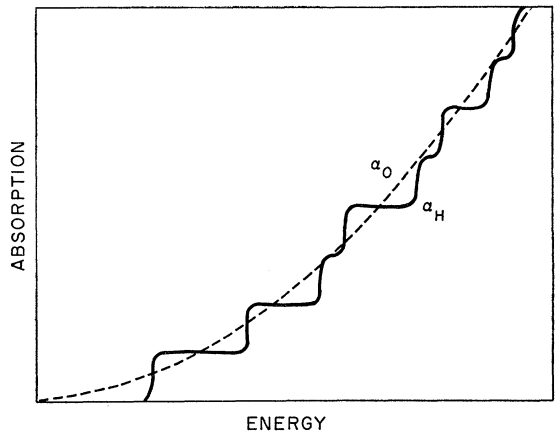

FIG. 4. Absorption coefficient as a function of energy for indirect transitions between two simple bands. This was constructed for $\omega_{c1}/\omega_{c2}=4/7$.

in this case that high resolution and low temperatures as well as polarized radiation will be necessary.

B. Indirect Transitions

We now turn to the case of indirect transitions, which involve both a photon and a phonon. We consider here the virtual process in which the electron is first excited to an intermediate state by a photon in a vertical transition and then is scattered by a phonon into a final state in the conduction-band minimum away from $\mathbf{k}=0$.[16] For the nonmagnetic case, this type of transition has been studied theoretically by Bardeen, Blatt, and Hall[17] and experimentally by Macfarlane and Roberts.[18] We shall not attempt a completely rigorous treatment of the problem but shall mainly consider the change in absorption induced by the redistribution of states in each band due to the presence of a magnetic field. In the expression for α, Eq. (10), $|M|^2$ is now replaced by a second order expression involving both photon and phonon matrix elements. From a generalization of Eq. (9) in Bardeen, Blatt, and Hall,[17] we obtain the absorption coefficient

$$\alpha_{\pm}=\frac{4\pi e^2}{ncm^2\omega}\frac{1}{V^2}\sum_{IAF}\left(M_s^2\begin{Bmatrix}N_s+1\\N_s\end{Bmatrix}\delta_{\sigma A,\sigma F}\Big/(\mathcal{E}_A-\mathcal{E}_F)^2\right)$$
$$\times\left|\sum_{jp}\boldsymbol{\pi}_{jp}\cdot\boldsymbol{\varepsilon}\int f_j^{*I}f_p^{A}d\mathbf{r}\right|^2\delta(\mathcal{E}_F-\mathcal{E}_I\pm k\theta-\omega). \quad (21)$$

Here I, A, and F correspond to initial, intermediate, and final states, and we are assuming that the transition from I to A is parity-allowed. $M_s^2(N_s+1)$ and $M_s^2N_s$ are the phonon matrix elements squared, $k\theta$ is the phonon energy, and $+$ and $-$ refer to phonon emission and absorption, respectively. We have included conservation of spin explicitly in $\delta_{\sigma A,\sigma F}$.

If we use again the model of parabolic bands, the integral of Eq. (21) reduces to that of Eq. (9) which implies, in this case, that for each initial state, there is only one intermediate state. Furthermore, near the absorption edge, we can neglect the variation with I and F of all factors except the last, and the shape of the absorption edge is essentially determined by the quantity

$$\sum_{IF}\delta(\mathcal{E}_F-\mathcal{E}_I\pm k\theta-\omega).$$

The following result for simple bands can then be obtained for α with and without a magnetic field:

$$\alpha_{0\pm}=K_{\pm}(m_1m_2)^{\frac{3}{2}}(\omega\mp k\theta-\mathcal{E}_g)^2,$$
$$\alpha_{H\pm}=2K_{\pm}(eH/c)^2(m_1m_2)^{\frac{1}{2}}\sum_{nn'}F(\omega-\mathcal{E}_{nn'}), \quad (22)$$
$$\mathcal{E}_{nn'}=\mathcal{E}_g\pm k\theta+\omega_{c1}(n+\tfrac{1}{2})+\omega_{c2}(n'+\tfrac{1}{2}).$$

Here $F(\omega-\mathcal{E}_{nn'})$ is a unit step function and $K_{\pm}$ is a constant[18] analogous to K and K'. Thus the absorption consists of a series of discontinuities[19] which is illustrated in Fig. 4.

Equation (22) is valid for ellipsoids if a density of states mass is used; for the magnetic case the mass is that along the magnetic field, and can be shown to be $m_l\cos^2\theta+m_t\sin^2\theta$, where θ is the angle of H with the ellipsoidal axis, and m_l and m_t are the longitudinal and transverse masses. For a degenerate band edge such as the valence band of germanium, we must go back to Eq. (19a); the various discontinuities will now have heights depending on the valence level involved. These can be determined from the transition probabilities for the direct transition which will be discussed in the following section. Because there is no selection rule on n and n' in the indirect case, the expected spectrum is rather complicated. Furthermore, since the effect is not oscillatory, it is necessary to go to low temperatures and high resolution to observe it.

Magneto-absorption effects of the type shown in Fig. 4 have, in fact, been observed by Zwerdling, Lax, Roth, and Button[3] in germanium at 4.2° and 1.5°K, in addition to the exciton absorption which has been reported by Macfarlane, McLean, Quarrington, and Roberts.[20] The experimental results are consistent with the theoretical spectrum; the details of the comparison are given in ZLRB.[3]

IV. GERMANIUM

We now consider in detail the case of the direct transition in germanium. This is believed to be a

[16] The alternative process in which the photon excites an electron into the final state and the phonon scatters the hole into the initial state can be treated in a similar manner. This process is believed to be less important for germanium and silicon.

[17] Bardeen, Blatt, and Hall, *Proceedings of the Conference on Photoconductivity, Atlantic City, 1954* (John Wiley & Sons, Inc., New York, 1956), p. 146.

[18] G. G. Macfarlane and V. Roberts, Phys. Rev. **97**, 1714 (1955); **98**, 1865 (1955).

[19] For the case in which the direct part of the transition is not parity allowed, the result would be more complex, but would still involve discontinuities.

[20] Macfarlane, McLean, Quarrington, and Roberts, Phys. Rev. **108**, 1377 (1957).

transition allowed at $\mathbf{k}=0$ between the complex valence band and the spherical conduction-band minimum at $\mathbf{k}=0$. We see from the simple band model that in order to locate the absorption peaks, it is necessary to solve Eq. (15) only for $k_z=0$, where z is the direction of the magnetic field. We thus obtain a line spectrum for the allowed transitions which can be compared with experiment. Statistical weights will be assigned to each line, essentially from the square of the momentum matrix element for the transition involved.

A. Energy Levels

The problem of the energy levels in a magnetic field of a degenerate valence band such as germanium has been treated by Luttinger[6] and we shall make extensive use of his results. The valence band edge functions in the absence of spin-orbit interaction belong to the representation Γ_{25}^+ of the cubic group and transform as yz, xz, xy. The sixfold degeneracy (including spin) is split by spin orbit interaction into a fourfold and a twofold degenerate set. The fourfold group lies higher and is the one we are concerned with. In the absence of a magnetic field, this group splits into two twofold degenerate bands away from $\mathbf{k}=0$. In the presence of the magnetic field this degeneracy is lifted, so that there are four sets of hole levels. A schematic energy level diagram is shown in Fig. 5.

The band-edge wave functions are basis functions for an angular momentum of $\frac{3}{2}$:

$$\begin{aligned}
&m_J=\tfrac{3}{2}, && u_{10}=(1/\sqrt{2})(X+iY)\alpha;\\
&m_J=-\tfrac{1}{2}, && u_{20}=-[1/(6)^{\frac{1}{2}}][(X-iY)\alpha+2Z\beta];\\
&m_J=\tfrac{1}{2}, && u_{30}=-[1/(6)^{\frac{1}{2}}][(X+iY)\beta-2Z\alpha];\\
&m_J=-\tfrac{3}{2}, && u_{40}=(1/\sqrt{2})(X-iY)\beta.
\end{aligned} \tag{23}$$

Here α and β are up and down spin functions, X, Y, Z are the original p-like spatial functions and the m_J value has been indicated. The form of the set of four coupled equations in Eq. (15) can be determined by group theoretical considerations.[21] For the explicit form, the reader is referred to Luttinger and Kohn[5] and Luttinger.[6]

Equation (15) for this case has been solved approximately by Luttinger[6] for nearly spherical bands (and $k_z=0$) and in addition, an exact solution was found for the magnetic field in the [111] direction. We shall be interested mainly in the simpler approximate solution. The magnetic field is assumed to be in a $(1\bar{1}0)$ plane, and the coordinate system is rotated so that the z direction is the direction of the magnetic field, and the basis functions, Eq. (23), are now referred to the transformed system. The solutions to first order in the warping then fall into two sets; the details of the derivation can be found in reference 6. (See also Appendix B.)

[21] Dresselhaus, Kip, and Kittel, Phys. Rev. **98**, 368 (1955); hereafter referred to as DKK.

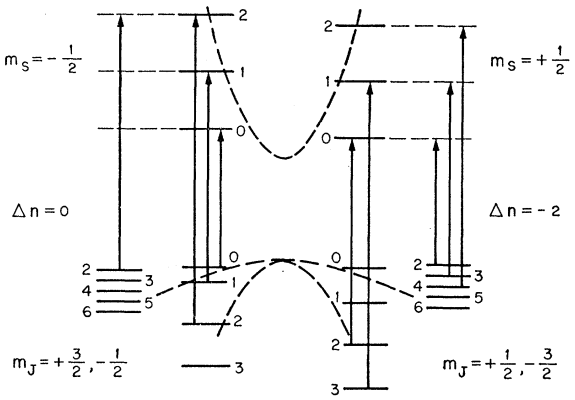

FIG. 5. Schematic diagram showing the magnetic levels for the valence and $\mathbf{k}=0$ conduction bands in germanium. The transitions shown are those allowed for $\mathbf{E}\|\mathbf{H}$.

$$\begin{aligned}
\text{Set (a):}\quad & f_{1a}(\mathbf{r})=a_1\Phi_{n-2}(\mathbf{r}),\\
& f_{2a}(\mathbf{r})=a_2\Phi_n(\mathbf{r}),\\
& f_{3a}(\mathbf{r})=f_{4a}(\mathbf{r})=0,
\end{aligned} \tag{24}$$

where, using the gauge of Eq. (4),

$$\Phi_n(\mathbf{r})=(L_yL_z)^{-\frac{1}{2}}\exp[ik_yy]\Phi_n(x-ck_y/eH). \tag{25}$$

Here the f_i refer to Eq. (15), and the wave functions are given by Eq. (18) with the band edge functions of Eq. (23). The energy level designated by n is thus a combination of n and $n-2$ harmonic oscillator states. a_1 and a_2 are the solutions of the equations

$$\begin{aligned}
&[(\gamma_1+\gamma')(n-\tfrac{3}{2})+\tfrac{3}{2}\kappa-\epsilon]a_1-\gamma''[3n(n-1)]^{\frac{1}{2}}a_2=0,\\
&-\gamma''[3n(n-1)]^{\frac{1}{2}}a_1\\
&\qquad+[(\gamma_1-\gamma')(n+\tfrac{1}{2})-\tfrac{1}{2}\kappa-\epsilon]a_2=0,
\end{aligned} \tag{26}$$

with the normalization condition $a_1^2+a_2^2=1$. The various parameters are defined below, and the normalized energy ϵ, defined by

$$\mathcal{E}=\mathcal{E}^0-(eH/mc)\epsilon, \tag{27}$$

is obtained by setting the determinant of Eq. (26) equal to zero:

$$\begin{aligned}
\epsilon_{a\pm}(n)=&\gamma_1 n-(\tfrac{1}{2}\gamma_1+\gamma'-\tfrac{1}{2}\kappa)\\
&\pm\{[-\gamma' n+(\tfrac{1}{2}\gamma'+\gamma_1-\kappa)]^2+3\gamma''^2n(n-1)\}^{\frac{1}{2}}.
\end{aligned} \tag{28}$$

Here for the $+$ signs, $n=0$, 1, $2\cdots$, and for the $-$ signs, $n=2$, 3, $4\cdots$. The $+$ and $-$ signs refer to light and heavy holes, respectively. Similarly, we have for the second set

$$\begin{aligned}
\text{Set (b):}\quad & f_{1b}(\mathbf{r})=f_{2b}(\mathbf{r})=0,\\
& f_{3b}(\mathbf{r})=b_1\Phi_{n-2}(\mathbf{r}),\\
& f_{4b}(\mathbf{r})=b_2\Phi_n(\mathbf{r}),
\end{aligned} \tag{29}$$

with $b_1^2+b_2^2=1$ and

$$[(\gamma_1-\gamma')(n-\tfrac{3}{2})+\tfrac{1}{2}\kappa-\epsilon]b_1-\gamma''[3n(n-1)]^{\frac{1}{2}}b_2=0,$$
$$-\gamma''[3n(n-1)]^{\frac{1}{2}}b_1+[(\gamma_1+\gamma')(n+\tfrac{1}{2})-\tfrac{3}{2}\kappa-\epsilon]b_2=0, \quad (30)$$

and for the energies

$$\epsilon_{b\pm}(n)=\gamma_1 n-(\tfrac{1}{2}\gamma_1-\gamma'+\tfrac{1}{2}\kappa)\pm\{[\gamma' n+(\gamma_1-\kappa-\tfrac{1}{2}\gamma')]^2+3\gamma''^2 n(n-1)\}^{\frac{1}{2}}, \quad (31)$$

with only the + sign for $n=0$, 1. Again + and − signs refer to light and heavy holes.

In the above equations, γ' and γ'' can be written

$$\gamma'=\gamma_3+(\gamma_2-\gamma_3)[(3\cos^2\theta-1)/2]^2,$$
$$\gamma''=\tfrac{2}{3}\gamma_3+\tfrac{1}{3}\gamma_2+\tfrac{1}{6}(\gamma_2-\gamma_3)[(3\cos^2\theta-1)/2]^2, \quad (32)$$

θ is the angle between the magnetic field and the z axis in the (110) plane. γ_1, γ_2, and γ_3 are valence band parameters which are related to other parameters in common use according to the definitions given in Table I. The classical (large n) cyclotron frequencies for the light and heavy holes are given in terms of these parameters by

$$\omega_{c\pm}\cong\frac{eH}{mc}[\gamma_1\pm(\gamma'^2+3\gamma''^2)^{\frac{1}{2}}]. \quad (33)$$

κ is a new constant introduced by Luttinger and necessary to describe the magnetic levels, although it is not measured in the classical cyclotron resonance experiments. Solutions in Eq. (28) and Eq. (31) correspond to that obtained from D_0 of Eq. (81) of reference 6.

Higher order terms in $\gamma_2-\gamma_3$, which is a measure of the warping of the energy surfaces, are obtained by using second order perturbation theory on the additional term D_1 of Eq. (81) in reference 6. This perturbing term shifts the levels slightly and, although we shall not go through the mathematical details,[22] this correction will be included where necessary in comparing the theory with experiment (Tables II–IV). Finally, Luttinger introduces a new parameter q, which affects the energy levels in the presence of spin-orbit interaction. We shall not include q in our calculation, as it is small.

TABLE I. Valence band parameters.

	L, M, N[a]	F, G, H_1, H_2[b]	A, B, C[c]
γ_1	$-\frac{1}{3}(L+2M)-1$	$-\frac{1}{3}(F+2G+2H_1+2H_2)-1$	A
γ_2	$-\frac{1}{6}(L-M)$	$-\frac{1}{6}(F+2G-H_1-H_2)$	$\frac{1}{2}B$
γ_3	$-\frac{1}{6}N$	$-\frac{1}{6}(F-G+H_1-H_2)$	$\frac{1}{2}(\frac{1}{3}C^2+B^2)^{\frac{1}{2}}$
κ		$-\frac{1}{6}(F-G-H_1+H_2)-\frac{1}{3}$	

[a] This notation is used by DKK (reference 21). Luttinger (reference 6) calls these A, B, and C.
[b] Sums of matrix elements as defined by DKK (reference 21) except that we have expressed F, G, H_1, and H_2 in units of $1/2m$ to make them dimensionless. See also Appendix B.
[c] This notation is used by DZL (reference 24) and DKK (reference 21).

[22] R. R. Goodman, doctoral dissertation, University of Michigan, 1958 (unpublished).

In addition to the valence band, we need the energy levels for the $\mathbf{k}=0$ conduction band minimum. Since this is spherical, the effective-mass Hamiltonian including spin will have the form

$$\mathcal{H}=\frac{1}{2m_c}\left(\mathbf{p}+\frac{e\mathbf{A}}{c}\right)^2+\mu^*\boldsymbol{\sigma}\cdot\mathbf{H}, \quad (34)$$

where $\boldsymbol{\sigma}$ is a Pauli spin vector and m_c is the conduction-band mass. With the inclusion of the effective magnetic moment μ^*, this is the most general form of $\mathcal{H}$ for a spherical band edge, as has been shown by Luttinger.[6] Since the conduction-band minimum is s like, it is not immediately obvious that μ^* should be different from the free-electron magnetic moment. However, it is shown in Appendix A that such an anomalous moment occurs because of the coupling of this band with the spin-orbit split valence band. The energy in this case is then given by

$$\mathcal{E}_c(n)=\frac{eH}{m_c c}(n+\tfrac{1}{2})\pm\mu^*H, \quad (35)$$

as shown schematically in Fig. 5. For the case of germanium, this effect should give a g value of -2.6 for the electron at $\mathbf{k}=0$, or a splitting of the magnetic levels of $1.3eH/mc$. The effect should be larger in InSb, as is discussed below.

The above results for the magnetic levels are valid when the energies are small compared to the separation of the band edges involved. This condition is usually satisfied in cyclotron resonance experiments, but with the large magnetic fields (40 kilogauss) used to observe the interband effects, marked deviations from quadratic behavior of the bands occurs. In the experiments of Zwerdling *et al.*[1–3] in Ge, oscillations were observed up to almost 0.2 electron volt beyond the energy gap. This is to be compared to 0.9 ev for the gap, and 0.3 ev for the spin-orbit splitting of the valence band. Consequently, it is necessary to go to higher than second order in $\mathbf{k}$ to compare the theory with experiment. The calculation of the levels for the conduction and valence bands is more complicated in this case, and the details are given in Appendix B.

B. Selection Rules and Transition Probabilities

The matrix element for an optical transition is, from Eq. (19),

$$M_\alpha=\frac{eE_0}{m\omega}\sum_i \mathbf{p}_{j\alpha}\cdot\boldsymbol{\varepsilon}\int f_j^*\Phi_{n'}d\mathbf{r}, \quad (36)$$

$$M_\beta=\frac{eE_0}{m\omega}\sum_i \mathbf{p}_{j\beta}\cdot\boldsymbol{\varepsilon}\int f_j^*\Phi_{n'}d\mathbf{r},$$

where j goes over the four degenerate valence band

edges, $\Phi_{n'}$ is the free electron wave function for the n'th level in the conduction band, and α and β indicate up and down spin, respectively, for the conduction band. We are neglecting the difference between $\boldsymbol{\pi}$ and $\mathbf{p}$ in Eq. (16) as this can be shown to be negligible. If we evaluate the matrix element for $k_z=0$, where the peaks in the absorption occurs, it can be seen from the form of the valence band wave functions, Eqs. (24) and (29), that the selection rules on n are $\Delta n=n'-n=0, -2$. Additional selection rules are obtained from the momentum matrix element between the band edge wave functions, e.g., $\mathbf{p}_{j\alpha}\cdot\boldsymbol{\varepsilon}=\langle u_{j0}|\,\mathbf{p}\cdot\boldsymbol{\varepsilon}\,|S\alpha\rangle$, where the u_{j0} are given by Eq. (23) and where S is the conduction band edge function, which transforms as $xyz(\Gamma_2^-)$ under the cubic group, and α is the spin-up function. From symmetry, we have for the spatial part of the matrix element

$$\langle X|\,p_x|S\rangle=\langle Y|\,p_y|S\rangle=\langle Z|\,p_z|S\rangle, \tag{37}$$

with all other combinations vanishing. From this and the orthogonality of the spin functions, a selection rule on m is obtained which is the same as that for the anomalous Zeeman effect, namely $\Delta m=m_s-m_J=0$ for polarization parallel to the magnetic field, and $\Delta m=\pm 1$ for polarization perpendicular to the magnetic field. The manner in which these selection rules are combined is shown by the following scheme indicating the combination of m_J and n values for the a and b sets in the valence band, and the m_s values for the conduction band:

$$\text{(a)}\begin{cases} n-2 & \tfrac{3}{2} & & \\ & \tfrac{1}{2} & n-2 & \\ n & -\tfrac{1}{2} & & \end{cases}\text{(b)}\qquad \begin{matrix} m_s \\ n'\alpha \quad \tfrac{1}{2} \\ n'\beta \quad -\tfrac{1}{2}. \end{matrix}$$

From the square of the matrix element, Eq. (36), it is also possible to calculate relative statistical weights for the various transitions. For example, for the transition from a level of set a to the spin-up conduction band, with $n'=n-2$, we find

$$|M_\alpha|^2\propto|\langle X|\,p_x|S\rangle|^2|a_1^2|\,(\epsilon_x-i\epsilon_y)/\sqrt{2}\,|^2. \tag{38}$$

Here the first factor is a constant; a_1, the amplitude of the $(n-2)$ harmonic oscillator state, will depend on the particular valence level, and we have, in addition, a factor depending on the polarization. The relative statistical weights found in this manner for the various allowed transitions are given in Table II for different polarizations of the incident radiation. From Table II for example it is apparent that for $\mathbf{E}\perp\mathbf{H}$ the light-hole transition $\bar{a}_+\alpha n'$ is 9 times as intense as light-hole transition $a_+\alpha n'$ and the corresponding heavy-hole transitions are of equal intensity. The relative intensities of other transitions are similarly determined. It is apparent from Table II that the use of polarized radiation greatly simplifies the spectrum and aids in identifying the various transitions.

Thus far we have not included the density of states weighting factor $[m_1m_2/(m_1+m_2)]^{\frac{1}{2}}$ resulting from Eqs. (11) and (13) for simple bands. In estimating this for germanium, we shall use an average heavy- or light-hole mass. For the heavy hole and electron $m_1\cong 0.3m$, $m_2\cong 0.04m$; hence the above weighting factor is approximately $\sqrt{m_2}$. For the light hole to electron, $m_1\cong m_2\cong 0.04m$ so that we have $0.7\sqrt{m_2}$ for this factor. Thus the density of states has relatively little effect on the intensities, as compared to the quantities listed in Table II. This fact justifies the use of the simple band approximation here.[23]

C. Numerical Results

A theoretical calculation was carried out for germanium using the values of the valence band cyclotron resonance parameters from Dexter, Zeiger, and Lax[24]:

$$A=13.1,\quad B=8.3,\quad C=12.5;$$

converting these to Luttinger's notation, we have

$$\gamma_1=13.1,\quad \gamma_2=4.15,\quad \gamma_3=5.5.$$

The three constants are sufficient to determine the three quantities F, G, and H_1, introduced by Dresselhaus, Kip, and Kittel,[21] which measure the effect of Γ_2^-, Γ_{12}^-, and Γ_{15}^- band edges on the valence band edge. We are neglecting H_2 which measures the effect of Γ_{25}^- band edges because, theoretically, these should be remote.[21] With the same assumption, the additional parameter $\kappa=3.23$ can be obtained from Table I.

With a knowledge of the energy gap ($\mathcal{E}_g=0.90$ electron volt) and the spin-orbit splitting ($\Delta=0.29$ ev), the conduction-band mass can be calculated from Eq. (A-4), if we assume that no Γ_{25}^+ bands except the valence band enter the picture. The result is

$$m/m_c=27.1.$$

TABLE II. Statistical weights.[a]

Transition	$\mathbf{E}\parallel\mathbf{H}$	$\mathbf{E}\perp\mathbf{H}$ Plane pol.	$\mathbf{E}\perp\mathbf{H}$ +Circ. pol.	$\mathbf{E}\perp\mathbf{H}$ −Circ. pol.
$\bar{a}_\pm\alpha n'$	0	$\frac{3}{4}a_1^2$	$\frac{3}{2}a_1^2$	0
$a_\pm\alpha n'$	0	$\frac{1}{4}a_2^2$	0	$\frac{1}{2}a_2^2$
$a_\pm\beta n'$	a_2^2	0	0	0
$\bar{b}_\pm\alpha n'$	b_1^2	0	0	0
$\bar{b}_\pm\beta n'$	0	$\frac{1}{4}b_1^2$	$\frac{1}{2}b_1^2$	0
$b_\pm\beta n'$	0	$\frac{3}{4}b_2^2$	0	$\frac{3}{2}b_2^2$

[a] The transitions are labeled by the valence band set $a_\pm$, $b_\pm$, where $+$ and $-$ refer to light and heavy holes, by the spin for the conduction band α or β, and by the quantum number n' for the conduction band. $\Delta n=-2$ transitions have bars over a or b; $\Delta n=0$ transitions do not. Thus $\bar{a}_+\alpha n'$ represents the transition from the $n'+2$ light hole level of set a to the n' level of the spin-up conduction band. To give orders of magnitude for high quantum numbers, from Eqs. (25), (26) and (28), (29), we have $a_1^2\approx 3a_2^2$ and $b_2^2\approx 3b_1^2$ for the light hole, with the opposite relations holding for the heavy hole. We have not included $[m_1m_2/(m_1+m_2)]^{\frac{1}{2}}$.

[23] For the case $\gamma_2=\gamma_3=\gamma_1-\kappa$, a linear expression for the energy as a function of n and k_z^2 can be obtained for the four sets of hole levels, so that this result would be exact for this case.

[24] Dexter, Zeiger, and Lax, Phys. Rev. **104**, 637 (1956); hereafter referred to as DZL.

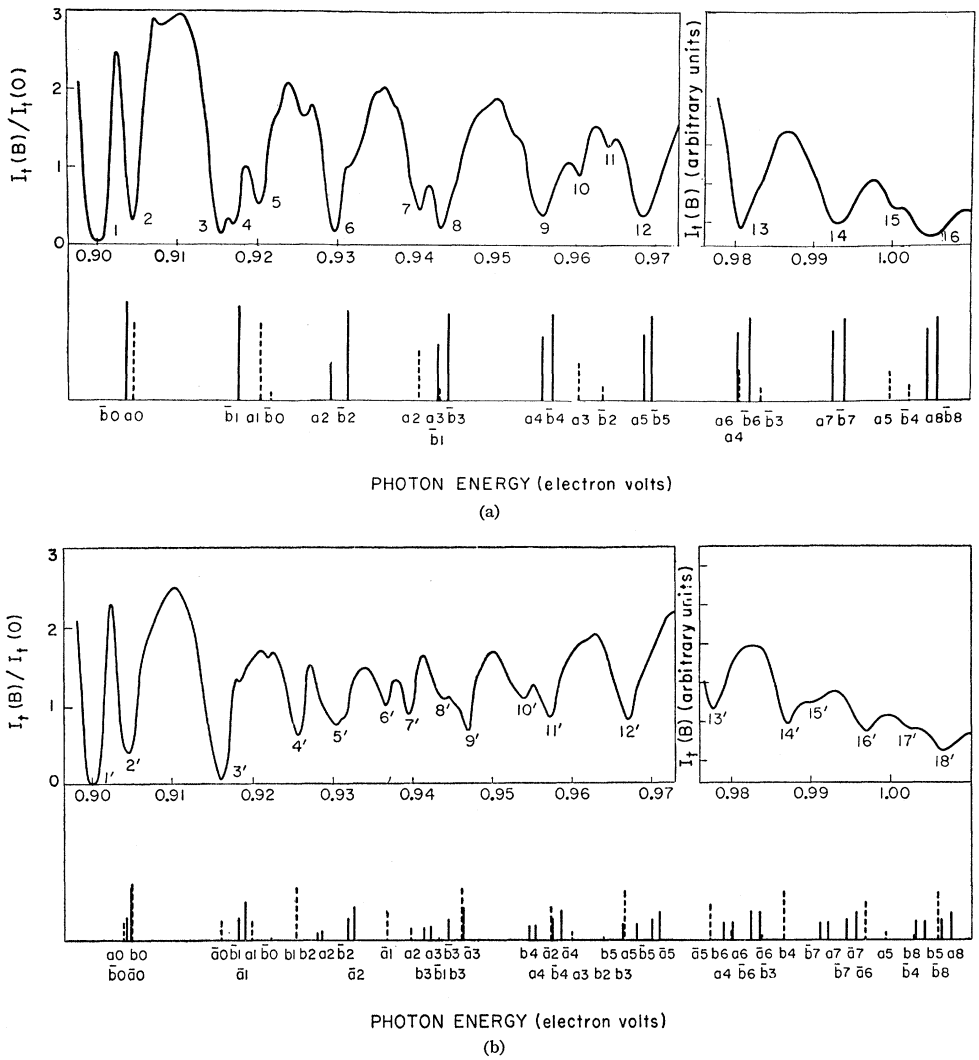

FIG. 6. Comparison of the theoretical spectrum with the results of Zwerdling, Lax, Roth, and Button[3] for (a) $\mathbf{E}\|\mathbf{H}$ and (b) $\mathbf{E}\perp\mathbf{H}$. The magnetic field is 38.9 kilogauss along [100] axis. The solid lines represent heavy-hole transitions and the dashed line, light-hole transitions. The lines are labeled with a simplification of the notation in Table II. The quantum number is that for the conduction band (spin is evident from Table II) and the subscript $\pm$ has been omitted.

In calculating k^4 and higher corrections to the levels, we make the additional assumption that the Γ_{15}^- and Γ_{12}^- bands are separated from the bands of interest by an energy much greater than $\mathcal{E}_g$. With these assumptions, the three cyclotron resonance parameters and the two energies determine the spectrum, as shown in Appendix B.

The calculation of the valence and $\mathbf{k}=0$ conduction-band levels was carried out for $H=38.9$ kg in the [100] and [111] directions. The corresponding line spectrum

TABLE III. Comparison of experiment and theory for heavy-hole transitions in germanium.

(1) n	(2)[a] $\epsilon_c(n)$[100]	(3) $\epsilon_c(n)$[100] $-\epsilon_c(n)$[111]	(4) $\epsilon_{a-}(n)$[100]	(5) $\epsilon_{b-}(n+2)$ [100]	(6)[b] Experiment	(7) Line	(8) $\epsilon_{a-}(n)$[111] $-\epsilon_{a-}(n)$[100]	(9) $\epsilon_{b-}(n+2)$[111] $-\epsilon_{b-}(n+2)$[100]	(10) Experiment
0	13.6∓0.65	0		2.2	2.7	2		−0.8	0.4
1	40.2∓0.6	−0.1		6.4	4.1	4		−1.6	−1.4
2	66.2∓0.6	−0.1	4.7	10.5	5.3	6	−2.0	−2.7	−2.0
3	91.6∓0.6	−0.3	9.5	13.2	10.0	8	−2.6	−2.5	−2.8
4	116.5∓0.55	−0.5	13.7	17.3	13.0	9	−3.5	−3.8	−3.6
5	140.5∓0.5	−0.7	17.9	21.1	17.3	12	−4.7	−4.7	−4.7
6	164.2∓0.5	−0.9	20.6	24.8	21.1	13	−4.5	−5.6	−5.3
7	187.4∓0.5	−1.2	24.3	28.5	25.3	14	−5.3	−6.5	−7.2
8	210.1∓0.5	−1.4	28.4	32.2	28.8	16	−6.6	−7.4	−8.1

[a] Minus and plus refer to up and down spin, respectively.
[b] Result of subtracting column (2) from the experimental line referred to in column (7).

for **H** in the [100] direction and for polarization ∥ and ⊥ to **H** is shown in Figs. 6(a) and 6(b) in comparison with the experimental results of Zwerdling, Roth, Lax and Button.[7,3] In order to obtain the fit shown, the theoretical spectrum was stretched[25] by 1.11% and the band edge was taken at 0.9870 electron volt. It can be seen that all the prominent minima are accounted for, except for lines 1, 1′, 3, 3′, which are believed to be due to exciton absorption.[7,3] The detailed calculation essentially verifies the preliminary identification of the prominent minima in Fig. 1 of reference 7.

For **E**∥**H** [Fig. 6(a)], the prominent transmission minima correspond to transitions from heavy-hole levels, and the theory indicates that these are unresolved doublets. The weaker light-hole transitions show up when they do not overlap the strong lines, as can be seen for lines 10 and 11. For **E**⊥**H** [Fig. 6(b)] the light-hole transitions appear more strongly, and two distinct series can be seen corresponding to transitions from the two sets of light-hole levels. These are $\bar{a}_+\alpha n'$ and $b_+\beta n'$. The experimental results indicate that the light-hole transitions in this case are even more intense relative to heavy-hole lines than the theory predicts; this disagreement is probably due to the relatively crude assumptions used for the statistical weights, since neither the detailed shape of the absorption edges nor the effect of k^4 terms on the amplitudes were considered.

A detailed comparison of theory and experiment for the heavy-hole doublets in the parallel spectrum is given in Table III. Column 2 gives the calculated electron levels for the [100] direction. If these are subtracted from the experimental line positions, the result (column 6) for a particular n should be the average of $\epsilon_{a-}(n)$ and $\epsilon_{b-}(n+2)$ which are given in columns 4 and 5. The experimental values were, for the most part, taken from a more recent run than those in Fig. 6, and the band-edge position was taken at 0.9868 electron volt. The experimental values do indeed lie between the two theoretical results, although slightly below the average position. When it is considered that the 90% of the line position due to the electron has been subtracted off, the agreement is certainly satisfactory.

The decrease in spacing of the heavy-hole doublets at the higher energies, due entirely to the electron, is evident from Fig. 6(a). The calculation shows that the electron level for $n=8$ lies 10% below the first order result, and that the mass has increased by almost 20%.

The calculation was carried out also for **H** in the [111] direction, and the difference between the levels in the two directions, which is a measure of the anisotropy is given in columns 8 and 9, for comparison with the experimental results in column 10. In obtaining these, account was taken of the small anisotropy in the electron levels (column 3), which is due to k^4 terms in the energy (Appendix B). If this were left out, the agreement would not be as good, although the difference is not great.

[25] Thus the parameters actually used are $\gamma_1=13.245$, $\gamma_2=4.20$, $\gamma_3=5.56$, $\kappa=3.266$.

TABLE IV. Comparison of experiment and theory for light-hole (a set) transitions in germanium.

(1)	(2)	(3) $\epsilon_{a+}(n)$[100]		(4)	(5)	(6) $\epsilon_{a+}(n)$[111]−$\epsilon_{a+}(n)$[100]		(8)
n	First order in H	Theory	Experiment	Line	First order in H	Theory	Experiment
0	2.8	2.8	1.4	2	−0.6	−0.6	+0.4
1	11.4	11.3	9.5	5	−1.5	−1.4	−2.1
2	30.2	29.3	28.7 28.8	7′ 7	−1.6	−1.9	−1.7 −1.7
3	51.3	48.7	48.0 48.4	6′ 10	0	−0.6	−0.5 +0.1
4	73.5	68.3	68.1	11′	1.1	0.0	0.0
5	95.9	87.3	87.9 87.9	13′ 15	2.2	0.6	+0.3 ...
6	118.4	105.7	105.7	16′	3.3	0.9	+2.2

Table IV. Comparison of experiment and theory for light-hole (a set) transitions in germanium.

A similar comparison between theory and experiment for the light-hole lines, principally found in the perpendicular spectrum, is given in Tables IV and V. Here a more direct comparison can be made, as the lines are singlets (except for 2 and 2′). In Table IV for the a set, comparison of columns 2 and 3 shows that the deviation from the first-order result for light-hole levels is greater than for the electron; this is due to the effect of the split-off band. The experimental values were again obtained by subtracting off the theoretical result for the electron. The agreement is good for the a set; for the b set (Table V) the theoretical values are slightly too low. It should be pointed out that the anisotropy of the light-hole lines, that is, the absolute energy shift, is as pronounced in this experiment as it is for the heavy-hole transitions, and the light-hole lines are well resolved. In cyclotron resonance the anisotropy of the heavy hole on a percentage basis was much larger than that of the light hole. Hence, once the lines are identified, one can use the light-hole anisotropy in evaluating the energy surface parameters just as was done for the heavy hole from cyclotron resonance.

Once the lines have been identified, it is possible to obtain experimental values of the conduction-band mass and g factor. For the g factor, if we assume that lines

TABLE V. Comparison of experiment and theory for light-hole (b set) transitions in germanium.

(1)	(2)	(3) $\epsilon_{b+}(n)$[100]		(4)	(5)	(6) $\epsilon_{b+}(n)$[111]−$\epsilon_{b+}(n)$[100]		(8)
n	First order in H	Theory	Experiment	Line	First order in H	Theory	Experiment
0	3.5	3.5	1.4	2′	1.6	1.6	1.0
1	22.1	22.0	22.2	4′	1.4	1.3	2.0
2	43.1	41.9	43.0	9′	3.0	2.8	2.8
3	65.2	62.1	63.3	12′	4.2	3.8	3.6
4	87.5	81.8	82.4 83.0	14′ 11	5.3	4.5	4.1 ...
5	110.1	100.6	102.0	18′	6.4	5.2	5.8

Table V. Comparison of experiment and theory for light-hole (b set) transitions in germanium.

7 and 7′ represent transitions from $\epsilon_{a+}(2)$ in the valence band to $\epsilon_c(2,\alpha)$ and $\epsilon_c(2,\beta)$, respectively, in the conduction band, the separation of 0.0007(0) electron volt gives a g factor of -3.1 for the data in Fig. 6, and -2.5 for the data from which the results in Tables III–V were obtained. The theoretical value is -2.60 for low fields; due to the change in curvature this should decrease in magnitude to -2.36 for $n=2$. There is some uncertainty in the identification since the intensities appear to be wrong in the $\perp$ case, although as pointed out earlier, we may rely more on the theoretical energies than on the intensities. The separation between the exciton lines 3 and 3′ may also be due to the conduction band spin splitting; these would give a g value of $(\pm)$ 3.7 for the [100] data and $(\pm)$ 2.3 for the [111] data.

For the conduction band mass, we can use the pairs of lines $a_+\beta 3$ and $\bar{a}_+\alpha 1$, $b_+\beta 4$ and $\bar{b}_+\alpha 2$, $a_+\beta 5$ and $\bar{a}_+\alpha 3$ to give the following values for differences between the electron levels:

$$\begin{aligned}\epsilon_c(3,\alpha)-\epsilon_c(1,\beta)&=52.9,\\ \epsilon_c(4,\alpha)-\epsilon_c(2,\beta)&=50.9,\\ \epsilon_c(5,\alpha)-\epsilon_c(3,\beta)&=50.2.\end{aligned}\tag{39}$$

Using these results and the experimental g value of 2.5, the energy levels can be fitted to the expression

$$\epsilon_c(n)=[27.1\pm 1](n+\tfrac{1}{2})-[0.33\pm 0.1](n+\tfrac{1}{2})^2\mp 0.6. \tag{40}$$

The first term here gives the value of the effective mass at $\mathbf{k}=0$, and the second, the change in curvature of the band. The third term gives the spin splitting where the $\mp$ refers to spin-up and spin-down, respectively. The effective mass agrees well with the result from the valence-band parameters. The theoretical value of the coefficient of the second term is 0.37; the theory actually indicates that a term cubic in n is significant at $n=5$.

V. INDIUM ANTIMONIDE

Infrared magneto-absorption experiments[2] have also been carried out on InSb at room temperature and the results indicate that a direct transition is involved similar to that in germanium. Four transmission minima were observed, whose positions in one run at 36.9 kilogauss were 0.1895, 0.2005, 0.2225, and 0.2475 electron volt. Relative to the gap of 0.180 ev obtained by extrapolation, these become 22, 48, 100, and 158 in units of eH/mc. Cyclotron resonance experiments give an effective mass for the conduction band at about 40 kilogauss of $m/70$ within 5%. Using this result, together with the energy gap and an estimate by Kane[26] of 0.9 electron volt for the spin-orbit splitting of the valence bands, the effective magnetic moment of the conduction band is found to be $-25\mu_0$ from Eq. (A-4). This corresponds very closely to the separation of the first two minima, which is $26eH/mc$. We therefore interpret the minima as transitions to the spin-up and spin-down conduction band from the lowest levels of the valence-band Landau levels with $n=0$. The average position gives an effective reduced mass of $m/70$, which is in good agreement with the cyclotron resonance result for the electron although the exact correspondence is fortuitous. The contribution from the valence band should be small, corresponding to the heavy hole. In a previous publication,[2] the second two minima were interpreted as due to transitions to $n=1$, spin-up and spin-down, in the conduction band. However, the separation between these two minima is too large by a factor of two. A more likely interpretation is that these correspond to $n=1$ and $n=2$ in the conduction band, for the predominant heavy-hole transition, and that the spin splitting does not appear because either it is not resolved or it is masked by complications from the valence band. The separations between the mean of the first two lines and the third line, and between the third and fourth lines, are 65 and 58 eH/mc, respectively, which are reasonably near the experimental cyclotron frequency, with the decrease probably due to change in curvature of the band. It is hoped that experiments at low temperatures and high resolution will reveal fine structure, and so give information about the structure of the valence band.

The experiment supports the theoretical prediction that the effective gyromagnetic ratio for the conduction electrons in InSb is about 50. It would be interesting to see if this could be observed by means of spin resonance. An estimate of the effect of the large magnetic moment on the susceptibility indicates that it is probably not significant, as the Landau diamagnetism dominates the Pauli paramagnetism even in this case.

VI. DISCUSSION

From the results in Ge, it appears that the effective-mass approximation and its extension to higher order in $\mathbf{k}$ give us a fairly good understanding of the magneto-absorption effects observed in semiconductors. The quantum effects predicted by Luttinger and Kohn[5] for the valence band in Ge are clearly demonstrated by these experiments. The fact that it was necessary to go to higher order in $\mathbf{k}$ indicates that the technique can be used to explore rather deeply into the bands. While this gives us additional information, it unfortunately complicates the experimental determination of band-edge parameters. It was for this reason that the cyclotron resonance values were used in the calculation with only a scale factor for fitting. It appears that a better fit could be obtained by using slightly different parameters. If such calculations are carried out, it may be possible to take κ and m_c as independent parameters, although it appears that this will not make a great deal of difference.

An interesting consequence of the results in germanium is the good agreement between the experimental conduction-band mass and the value calculated

[26] E. O. Kane, J. Phys. Chem. Solids **1**, 249 (1957).

from the valence-band masses. The relationship between the masses was obtained on the basis of the one-electron approximation. Actually the inclusion of an exchange operator in the one-electron Hamiltonian has been shown by Kane[27] to alter this relationship, although Kane's estimate of this effect in germanium shows that the calculated conduction-band mass would be changed by only a few percent, and this is probably within the uncertainty of the experimental results. The concept of an effective mass is valid from a many-electron standpoint, as has been shown by Kohn,[28] but it is not obvious that the valence- and conduction-band masses should be related in the same way as for independent electrons. It was also found that the change in curvature of the bands agreed well with the one-electron theory. Thus it appears that while many-electron effects may alter the magnitudes of the parameters and the energy gaps involved, the relationships between them are maintained to a good approximation in the range of energies studied. The appearance of exciton lines is of course due to many-electron effects.

We have been more exact in the calculation of energy levels than of intensities. Detailed calculations of line shapes would involve evaluation of the squared amplitudes and the one-dimensional density of states as a function of k_z, and would be rather involved. There do exist additional allowed transitions for $k_z \neq 0$, but since there is no singularity in the absorption, we would not expect these to show up as absorption peaks experimentally; they may, however, appear as shoulders. There should also exist additional "forbidden" transitions due to the warping of the energy surfaces in the valence band, and related to the harmonics observed in cyclotron resonance. This may account for some of the weaker absorptions. Another source for extra lines is exciton absorption; the effect of the magnetic field is to pull the exciton lines up into the band (e.g., lines 3 and 3′ in Fig. 6) and to intensify them.[7]

The optical magneto-absorption technique is useful for exploring band edges not available for cyclotron resonance because of the lack of carriers, as in the $\mathbf{k}=0$ conduction band in Ge. The results confirm the theoretical predictions as to the symmetry (Γ_2^-) of this band. There has been some question from the optical absorption as to whether the direct transition is parity-allowed, due to the shape of the absorption edge.[12] Departure from the theoretical $(\omega-\mathcal{E}_g)^{\frac{1}{2}}$ dependence may be due to exciton absorption[7] and to optical phonon effects.[29]

ACKNOWLEDGMENTS

The authors wish to thank Dr. H. J. Zeiger and Dr. G. W. Pratt for interesting and helpful discussions.

[27] E. O. Kane, J. Phys. Chem. Solids **6**, 236 (1958).
[28] W. Kohn, Phys. Rev. **105**, 509 (1957).
[29] W. P. Dumke, Phys. Rev. **105**, 139 (1957).

APPENDIX A. EFFECTIVE MAGNETIC MOMENT FOR SPHERICAL ENERGY BANDS

Equation (34) for the 2×2 effective-mass Hamiltonian for spherical bands can be obtained as a specialization of Eq. (15) in which we must be careful to maintain the orders of the factors[6] $\mathbf{P}$. The quantities $m^*=m_c$ and μ^* can be obtained from Eqs. (16) and (17). The term proportional to H comes from the noncommutivity of the x and y components of $\mathbf{P}$. The results are

$$\frac{1}{2m^*}=\frac{1}{2m}+\frac{1}{m^2}\sum_{m\neq 0}\frac{|p_{\alpha n}{}^x|^2}{\mathcal{E}^0-\mathcal{E}_n{}^0}, \tag{A-1}$$

$$\mu^*=\frac{e}{2mc}+\frac{e}{2m^2c}\frac{1}{i}\sum_{n\neq 0}\frac{p_{\alpha n}{}^x p_{n\alpha}{}^y-p_{\alpha n}{}^y p_{n\alpha}{}^x}{\mathcal{E}^0-\mathcal{E}_n{}^0}, \tag{A-2}$$

where $\mathbf{p}_{\alpha n}$ is the momentum matrix between the spin-up band edge and the nth band edge. The contribution of the second term in $\pi_{i\mu}$, Eq. (17), can be shown to be negligible.[30]

For the case of the split-off valence band in germanium, μ^* has been evaluated by Luttinger[6] and shown to be of the order of κ (Table I). For the spherical $\mathbf{k}=0$ conduction band, we can evaluate μ^* by assuming that the only band which makes a significant contribution is the valence band, which is split by spin orbit interaction into the fourfold and twofold bands, at energies $\mathcal{E}_g$ and $\mathcal{E}_g+\Delta$ below the $\mathbf{k}=0$ conduction band, respectively. The fourfold band edge wave functions are given by Eq. (23), while for the twofold band we have

$$\begin{aligned} u_{50}&=\frac{1}{\sqrt{3}}[(X+iY)\beta+Z\alpha], \\ u_{60}&=\frac{1}{\sqrt{3}}[(X-iY)\alpha-Z\beta]. \end{aligned} \tag{A-3}$$

Substituting these wave functions into Eqs. (A-1) and (A-2) and using $S\alpha$ for the spin-up conduction band, we find

$$\begin{aligned} \frac{1}{2m^*}&=\frac{1}{2m}+\frac{1}{m^2}\frac{3\mathcal{E}_g+2\Delta}{3\mathcal{E}_g(\mathcal{E}_g+\Delta)}|\langle S|p_x|X\rangle|^2, \\ \mu^*&=\frac{e}{2mc}-\frac{e}{m^2c}\frac{\Delta}{3\mathcal{E}_g(\mathcal{E}_g+\Delta)}|\langle S|p_x|X\rangle|^2, \end{aligned} \tag{A-4}$$

μ^* can also be written in terms of m^*, as follows

$$\mu^*=\frac{e}{2mc}\left[1-\left(\frac{m}{m^*}-1\right)\frac{\Delta}{3\mathcal{E}_g+2\Delta}\right]. \tag{A-5}$$

APPENDIX B. HIGHER ORDER TERMS IN THE ENERGY

The effective mass approximation can be generalized to include terms of higher order than 2 in k, as has been

[30] E. O. Kane, J. Phys. Chem. Solids **1**, 82 (1956).

discussed by Kjeldaas and Kohn.[31] The general expression for the effective-mass Hamiltonian can be written

$$\mathcal{H}_{ij}^{\text{eff}}=\mathcal{H}_{ij}+\sum_{\mu}\frac{\mathcal{H}_{i\mu}'\mathcal{H}_{\mu j}'}{\mathcal{E}-\mathcal{E}_{\mu}^{0}}+\sum_{\mu\nu}\frac{\mathcal{H}_{i\mu}'\mathcal{H}_{\mu\nu}'\mathcal{H}_{\nu j}'}{(\mathcal{E}-\mathcal{E}_{\mu}^{0})(\mathcal{E}-\mathcal{E}_{\nu}^{0})}$$
$$+\sum_{\mu\nu\lambda}\frac{\mathcal{H}_{i\mu}'\mathcal{H}_{\mu\nu}'\mathcal{H}_{\mu\lambda}'\mathcal{H}_{\lambda j}'}{(\mathcal{E}-\mathcal{E}_{\mu}^{0})(\mathcal{E}-\mathcal{E}_{\nu}^{0})(\mathcal{E}-\mathcal{E}_{\lambda}^{0})}+\cdots, \quad \text{(B-1)}$$

where i and j refer to the degenerate band edge considered, and u, ν, λ are all other band edges. This expression is more compact than that used by Kjeldaas and Kohn,[31] and the final energy appears in the denominator. Using $\mathbf{P}=\mathbf{p}+e\mathbf{A}/c$, we have

$$\mathcal{H}_{ij}=\left[\mathcal{E}_{i}^{0}\delta_{ij}+\frac{\mathbf{P}^{2}}{2m}\delta_{ij}+\mu_{0}(\boldsymbol{\sigma}\cdot\mathbf{H})_{ij}\right], \quad \text{(B-2)}$$

$$\mathcal{H}_{i\mu}'=\frac{1}{m}\mathbf{P}\cdot\boldsymbol{\pi}_{i\mu}, \quad \text{(B-3)}$$

$$\mathcal{H}_{\mu\nu}'=\frac{1}{m}\mathbf{P}\cdot\boldsymbol{\pi}_{\mu\nu}+\frac{1}{2m}\mathbf{P}^{2}\delta_{\mu\nu}+\mu_{0}(\boldsymbol{\sigma}\cdot\mathbf{H})_{\mu\nu}. \quad \text{(B-4)}$$

The last two terms in Eq. (B-4) are unimportant when the effective masses are small. In evaluating Eq. (B-1) for the magnetic case, we must be careful to maintain the order of the factors[6] of $\mathbf{P}$.

In evaluating Eq. (B-1) for the valence (Γ_{25}^{+}) and $\mathbf{k}=0$ conduction (Γ_{2}^{-}) bands of germanium, we shall assume that all other band edges are far removed from these two, where we now include the split-off band with the valence band. Thus we can neglect $\mathcal{E}$ in the denominator unless it appears with an energy of the order of the gap or the spin-orbit splitting. For the conduction band, we make the additional assumption that it interacts only with the valence band. We shall neglect the last term in Eq. (B-4) and include the second term approximately by replacing $\mathcal{E}$ by $\mathcal{E}'=\mathcal{E}-(n+\frac{1}{2})eH/mc$ in the denominator. The third term of Eq. (B-1) vanishes from symmetry, and we have

$$\mathcal{H}_{ij}'=\left(\mathcal{E}_{0}+\frac{P^{2}}{2m}\right)\delta_{ij}+\mu_{0}(\boldsymbol{\sigma}\cdot\mathbf{H})_{ij}+\frac{1}{m^{2}}\sum_{\mu}\frac{\mathbf{P}\cdot\boldsymbol{\pi}_{i\mu}\mathbf{P}\cdot\boldsymbol{\pi}_{\mu j}}{\mathcal{E}'-\mathcal{E}_{\mu 0}}$$
$$+\frac{1}{m^{4}}\sum_{\mu\nu\lambda}\frac{(\mathbf{P}\cdot\boldsymbol{\pi}_{i\mu})(\mathbf{P}\cdot\boldsymbol{\pi}_{\mu\nu})(\mathbf{P}\cdot\boldsymbol{\pi}_{\nu\lambda})(\mathbf{P}\cdot\boldsymbol{\pi}_{\lambda j})}{(\mathcal{E}'-\mathcal{E}_{\mu 0}^{0})(\mathcal{E}'-\mathcal{E}_{\nu 0}^{0})(\mathcal{E}'-\mathcal{E}_{\lambda 0}^{0})}. \quad \text{(B-5)}$$

Here μ and λ run over the 6 valence band functions. Except for the last term, the expressions are those in Appendix A [Eq. (A-4)], except that $\mathcal{E}_{g}$ is replaced by $\epsilon+\mathcal{E}_{g}^{0}$, where ϵ is the energy relative to the conduction band edge. The last term can be evaluated by noting that the expression

$$\frac{1}{m^{2}}\sum_{\nu}\frac{\mathbf{P}\cdot\boldsymbol{\pi}_{\mu\nu}\mathbf{P}\cdot\boldsymbol{\pi}_{\nu\lambda}}{\mathcal{E}-\mathcal{E}_{\nu}^{0}}$$

is just the part of the effective-mass Hamiltonian for the valence band arising from bands other than the conduction band. (We may let $\mathcal{E}'$ be the valence band edge $\mathcal{E}_{v}^{0}$, since we assume $\mathcal{E}_{v}^{0}$ to be far away.) This can be evaluated by the methods of DKK, using the constants (Table I)

$$F=\frac{2}{m}\frac{|\langle X|P_{x}|S\rangle|^{2}}{\mathcal{E}_{g}},$$

$$G=\frac{1}{m}\sum_{\mu(\Gamma_{12}^{-})}\frac{|\langle X|P_{x}|\mu\rangle|^{2}}{\mathcal{E}_{v}^{0}-\mathcal{E}_{\mu}^{0}}$$
$$=-\frac{2}{m}\sum_{\mu(\Gamma_{12})}\frac{\langle X|P_{x}|\mu\rangle\langle\mu|P_{y}|Y\rangle}{\mathcal{E}_{v}^{0}-\mathcal{E}_{\mu}^{0}}, \quad \text{(B-6)}$$

$$H_{1}=\frac{2}{m}\sum_{\mu(\Gamma_{15}^{-})}\frac{|\langle X|P_{y}|\mu\rangle|^{2}}{\mathcal{E}_{v}^{0}-\mathcal{E}_{\mu}^{0}}$$
$$=\frac{2}{m}\sum_{\mu(\Gamma_{15}^{-})}\frac{\langle X|P_{x}|\mu\rangle\langle\mu|P_{y}|Y\rangle}{\mathcal{E}_{v}^{0}-\mathcal{E}_{\mu}^{0}}.$$

These are essentially the constants used by DKK except that we have made them dimensionless by multiplying by $2m$. We are neglecting the difference between $\boldsymbol{\pi}$ and $\mathbf{P}$ (reference 30) and assuming that the band edges Γ_{25}^{-} make no contribution ($H_{2}=0$). The notation for the conduction and valence band edge functions is given in Appendix A.

The result for the last term in Eq. (B-5) is

$$-\frac{F\mathcal{E}_{g}}{2m^{2}}\left(\frac{1}{\mathcal{E}'+\mathcal{E}_{g}'}\right)^{2}$$
$$\times\{GP^{4}+(2H_{1}-3G)[P_{x}^{2}P_{y}^{2}+P_{x}^{2}P_{z}^{2}+P_{y}^{2}P_{z}^{2}]\}. \quad \text{(B-7)}$$

We have neglected the noncommutivity of the components of $\mathbf{P}$, as the result is important only for large n. $\mathcal{E}_{g}'$ is some average between $\mathcal{E}_{g}$ and $\mathcal{E}_{g}+\Delta$ (see Appendix A). We shall use the same average as in the effective mass. To obtain the contribution of Eq. (B-7) to the Landau level n, we shall take its expectation value and approximate for large n.

For the case of germanium, in which μ^{*}, Eq. (A-4) is small, we can first solve for the average Landau level for the two spins, and then add and subtract $\mu^{*}H$. The dominant term is the third term in Eq. (B-5). If only $\epsilon+\mathcal{E}_{g}$ appeared in the denominator, a quadratic equation would result for ϵ. It is convenient to use the solution to this quadratic equation and include the contribution from the split-off band by iteration. With some approximation, the resulting expression for the

[31] T. Kjeldaas, Jr., and W. Kohn, Phys. Rev. **105**, 806 (1957).

energy level for $k_z=0$ is then (expressing all energies in units of eH/mc)

$$\epsilon=\epsilon_1+\epsilon_2+\epsilon_3+\epsilon_4,$$

$$\epsilon_1=\tfrac{1}{2}\mathcal{E}_g\left\{\left(1+\frac{4\epsilon_0}{\mathcal{E}_g}\right)^{\frac{1}{2}}-1\right\},$$

$$\epsilon_0=-F(n+\tfrac{1}{2})\left(1-\frac{\Delta}{3(\epsilon_1+\mathcal{E}_g+\Delta)}\right),$$

$$\epsilon_2=n+\tfrac{1}{2},$$

$$\epsilon_3\cong-\frac{\epsilon_1^{\,2}}{F\mathcal{E}_g}\left[H_1+\tfrac{1}{2}G-\tfrac{1}{2}(H_1-\tfrac{3}{2}G)\left(\frac{3\cos^2\theta-1}{2}\right)^2\right], \quad \text{(B-8)}$$

$$\epsilon_4\cong\mp\tfrac{1}{2}\left[\frac{-F\mathcal{E}_g\Delta}{3(\epsilon_1+\mathcal{E}_g)(\epsilon_1+\mathcal{E}_g+\Delta)}-1\right].$$

Equations (B-8) actually give a somewhat better result than second order in n. ϵ_3 is anisotropic; we have evaluated it for H in a $(1\bar{1}0)$ plane, with θ the angle with the [001] axis.

For the valence bands, we shall neglect the fourth term in Eq. (B-1), as all the "v" bands for which the matrix elements exist are theoretically remote. This reduces the problem to that of solving the six effective-mass equations including the split-off bands, and in addition including ϵ in the denominators.

It is possible to obtain a solution for the 6×6 equations for nearly-spherical energy surfaces by a straightforward generalization of the method used by Luttinger.[6] The 6×6 effective-mass Hamiltonian (Eq. (15)) breaks up into two 3×3 matrices involving columns and rows 1, 2, 6 and 3, 4, 5, respectively, using the basis functions of Eqs. (21) and (A-3). Using the notation a and b to distinguish them, these can be shown to be

$$\text{set } a: \begin{bmatrix} (\gamma_1+\gamma')(N+\frac{1}{2})+3\kappa/2-\epsilon & -\sqrt{3}\gamma''a^2 & 6^{\frac{1}{2}}\gamma''a^2 \\ -\sqrt{3}\gamma''a^{\dagger 2} & (\gamma_1-\gamma')(N+\frac{1}{2})-\kappa/2-\epsilon & -\sqrt{2}[\gamma'(N+\frac{1}{2})-\frac{1}{2}(\kappa+1)] \\ 6^{\frac{1}{2}}\gamma''a^{\dagger 2} & -\sqrt{2}[\gamma'(N+\frac{1}{2})-\frac{1}{2}(\kappa+1)] & \Delta+\gamma_1(N+\frac{1}{2})-\epsilon \end{bmatrix}\begin{bmatrix} f_{1a} \\ f_{2a} \\ f_{6a} \end{bmatrix}=0, \quad \text{(B-9)}$$

$$\text{set } b: \begin{bmatrix} (\gamma_1-\gamma')(N+\frac{1}{2})+\kappa/2-\epsilon & -\sqrt{3}\gamma''a^2 & -\sqrt{2}[\gamma'(N+\frac{1}{2})+\frac{1}{2}(\kappa+1)] \\ -\sqrt{3}\gamma''a^{\dagger 2} & (\gamma_1+\gamma')(N+\frac{1}{2})-3\kappa/2 & 6^{\frac{1}{2}}\gamma''a^{\dagger 2} \\ -\sqrt{2}[\gamma'(N+\frac{1}{2})+\frac{1}{2}(\kappa+1)] & 6^{\frac{1}{2}}\gamma''a^2 & \Delta+\gamma_1(N+\frac{1}{2})-\epsilon \end{bmatrix}\begin{bmatrix} f_{3b} \\ f_{4b} \\ f_{5b} \end{bmatrix}=0, \quad \text{(B-10)}$$

where γ_1, etc., are defined in Table I and all energies are in magnetic units. $-\epsilon$ here is the energy relative to the valence band. Here we have used creation and annihilation operators $a^\dagger$ and a defined by

$$a^\dagger=(c/2e)^{\frac{1}{2}}(P_x+iP_y),$$
$$a=(c/2e)^{\frac{1}{2}}(P_x-iP_y), \quad \text{(B-11)}$$
$$\{a,a^\dagger\}\equiv N+\tfrac{1}{2}.$$

These have the following properties when operating on the harmonic oscillator functions Φ_n:

$$a^\dagger\Phi_n=(n+1)^{\frac{1}{2}}\Phi_{n+1}, \quad a\Phi_n=n^{\frac{1}{2}}\Phi_{n-1}. \quad \text{(B-12)}$$

From the relations (B-12), the solution for Eq. (B-9) is given by Eq. (24), with, in addition

$$f_{6a}=a_3\Phi_n(\mathbf{r}), \quad (f_{5a}=0).$$

Similarly for Eq. (B-10), we have Eq. (27), with

$$f_{5b}=b_3\Phi_{n-2}, \quad (f_{6b}=0).$$

By substituting these solutions in Eqs. (B-9) and (B-10), we obtain sets of linear equations for the a's and b's. The secular equation in each case is a cubic, and the following form is useful for iteration:

$$\epsilon_0=r_1-\frac{s_2^2+t^2}{d}\pm\left[\left(s_1-\frac{t^2-s_2^2}{d}\right)^2+t^2\left(1-\frac{2s_2}{d}\right)^2\right]^{\frac{1}{2}}, \quad \text{(B-13)}$$

where

$$d=\Delta+r_2-\epsilon_0, \quad \text{(B-14)}$$

and

set a	set b
$r_1=\gamma_1 n-(\frac{1}{2}\gamma_1+\gamma'-\frac{1}{2}\kappa)$,	$r_1=\gamma_1 n-(\frac{1}{2}\gamma_1-\gamma'+\frac{1}{2}\kappa)$,
$r_2=\gamma_1(n+\frac{1}{2})-(\kappa+\frac{1}{2})$,	$r_2=\gamma_1(n-\frac{3}{2})-(\kappa+\frac{1}{2})$,
$s_1=\gamma' n-(\frac{1}{2}\gamma'+\gamma_1-\kappa)$,	$s_1=\gamma' n+(\gamma_1-\kappa-\frac{1}{2}\gamma')$,
$s_2=\gamma'(n+\frac{1}{2})-\frac{1}{2}\kappa+1$,	$s_2=\gamma'(n-\frac{3}{2})+\frac{1}{2}\kappa+1$,
$t=-\sqrt{3}\gamma''[n(n-1)]^{\frac{1}{2}}$,	$t=-\sqrt{3}\gamma''[n(n-1)]^{\frac{1}{2}}$.

(B-15)

Equation (B-13) is used for light-hole levels; for the heavy-hole levels the effect of the split-off band can be neglected.

We must now include the variation of the energy denominators in γ_1, etc. If all the constants in Eq. (B-9) [or Eq. (5)] contained the factor $1/(\epsilon+\mathcal{E}_g)$, we could multiply the equation by $(1+\epsilon/\mathcal{E}_g)$, and would have the result

$$(1+\epsilon/\mathcal{E}_g)=\epsilon_0, \quad \text{(B-16)}$$

i.e., a quadratic equation, where ϵ_0 is given by Eq. (B-13). This result is almost valid, since the principle contribution to the valence band parameters is from the $\mathbf{k}=0$ conduction band, and we can make a small correction for the other band edges which we assume to be far away. We can then finally write for the energy

levels

$$\epsilon=\epsilon_1-(n+\tfrac{1}{2}),$$

$$\epsilon_1=\tfrac{1}{2}\mathcal{E}_g\left\{\left[1+\frac{4[\epsilon_0+(n+\tfrac{1}{2})+\epsilon_3+\epsilon_4]}{\mathcal{E}_g}\right]^{\frac{1}{2}}-1\right\}. \quad \text{(B-17)}$$

Here the $n+\frac{1}{2}$ appears from using $\mathcal{E}'$ in Eq. (B-5), and ϵ_0 is given by Eq. (B-13) with d redefined:

$$d=\Delta(1+\epsilon_1/\mathcal{E}_g)+r_2-\epsilon_0. \quad \text{(B-18)}$$

For ϵ_3, if the valence band effective mass Hamiltonian is $\mathcal{H}(F,G,H_1)$, using the parameters of Eq. (B-6), then

$$\epsilon_3=(\epsilon_1/\mathcal{E}_g)(\langle\mathcal{H}(0,G,H_1)\rangle+n+\tfrac{1}{2}), \quad \text{(B-19)}$$

where we can take the expectation value with respect to the wave functions in Eqs. (22) and (27) since this is a small correction.

Finally ϵ_4 is the contribution of D_1 in reference 4, and is obtained from second order perturbation theory, using Eqs. (22) and (27), since again this is a small correction.

PHYSICAL REVIEW VOLUME 114, NUMBER 1 APRIL 1, 1959

Optical Properties of Nickel and Tungsten and Their Interpretation According to Drude's Formula

S. ROBERTS
General Electric Research Laboratory, Schenectady, New York
(Received August 22, 1958)

New optical data are reported for nickel at 88°, 298°, and 473°K and for tungsten at 298°, 1100°, and 1600°K in the wavelength range 0.365 to 2.65 microns. These data are shown to depend on wavelength in a way which is in good quantitative agreement with a formula initially proposed by Drude. By attributing different terms in Drude's equation to the motion of different classes of free and bound electrons, one may conclude that several classes of each are present in both metals. Each class of free electrons accounts for a portion of the dc conductivity and has its own characteristic relaxation time or wavelength. From this analysis it appears that most of the dc conductivity may be attributed to one class of free electrons, although optical properties are strongly influenced by other classes as well. In both metals the characteristic wavelength λ_{r1} of the first class of free electrons proves to be proportional to the corresponding conductivity σ_1 at different temperatures. In nickel the constant ratio σ_1/λ_{r1} accounts for the low temperature coefficient of optical properties throughout the visible and near infrared range. In tungsten this constant ratio contributes to the existence of the x-point or cross-over wavelength in the spectral emissivity. It is shown that the anomalous skin effect may not be a significant factor in the measured optical properties of a metal like nickel in the range of wavelength where these properties have only a small temperature coefficient.

I. HISTORICAL ORIENTATION

OPTICAL properties of thick metal specimens may be measured most readily by reflected light. The principles for doing this were worked out many years ago and were carried to a high state of refinement by Drude.[1] Drude[2] also showed that the observed optical properties depended on wavelength in a rational manner. On the basis of this analysis he claimed that there were at least two kinds of charged particles which could move freely in the metals he studied. He called them "ions" but was unable to give a satisfactory theory to account for them. Nevertheless, Drude[3] did point out that other properties such as Hall effect and thermoelectric phenomena likewise indicated the presence of two kinds of charge carriers. Drude's "ion hypothesis," however, was not well received by his contemporaries. In a recent paper (hereafter referred to as paper I) the author[4] appears to have been the first since Drude to recommend that serious consideration be given to this interpretation of optical properties of metals.

In paper I and in the present work the author reports that the interpretation depending on the implied existence of more than one class of free electrons, distinguished by their different relaxation times, is highly successful in describing the optical properties *versus* wavelength of a variety of metals. One might wonder, perhaps, why such a simple fact has remained so long in obscurity. It may be that an appropriate reason is suggested in these words of Lucretius: ". . . no fact is so simple that it is not harder to believe than to doubt at the first presentation." The circumstances related below certainly indicate that the above fact was very difficult to believe in Drude's time.

Schuster[5] appears to have been the first to have suggested that, since electrons in a metal were the same as those observed in cathode rays, they should all have the same charge, the same mass, and in each metal a single relaxation time. In the absence of quantum mechanics this argument seemed quite logical. In

[1] P. Drude, Ann. Physik **39**, 481 (1890).
[2] P. Drude, Physik. Z. **1**, 161 (1900).
[3] P. Drude, Ann. Physik **1**, 566 (1900); **3**, 369 (1900); **7**, 687 (1902).
[4] S. Roberts, Phys. Rev. **100**, 1667 (1955).
[5] A. Schuster, Phil. Mag. **7**, 151 (1904).